

## Chapter 3

### Representational and Computational Properties of Resonance Information Encoded in a Standing Wave

We have seen that harmonic resonance is a unique pattern formation principle that can create a great variety of spatial patterns based on the twin principles of symmetry and periodicity, and those patterns are automatically sorted, or organized in an ordered hierarchical array, in which the simpler, more primal patterns correspond to the lower vibrational energies, while higher harmonics on those primal basis functions require progressively higher vibrational energies to sustain them. This is the ultimate origin of the Gestalt principle of *prägnanz*, the principle by which the simplest interpretation is the one most likely to be perceived, the perceptual counterpart to Occam's razor. In this chapter we explore those aspects of harmonic resonance that are conducive to exploitation as a computational and representational mechanism in the brain.

There are four distinct types of pattern information encoded in a standing wave. Falstad's Box Modes applet depicts the standing wave as a spatial field of varying magnitude and periodically reversing polarity, a sinusoidal type profile in three dimensions, as shown in Figure 3.1 A, for the same four standing wave patterns as in Figure 2.7. This corresponds to the function  $u(x,y,z)$  in the wave equation and in Falstad's Box Modes applet. In a Chladni plate, this corresponds to the instantaneous shape of the steel plate during vibration, or the degree of deviation from its central equilibrium configuration. This is the kind of signal that could be used to define continuous gradient type patterns, for example the continuous shading observed in the coloration of a Siamese cat, with its lighter belly blending smoothly with a darker back and extremities. In motor control, the analog magnitude signal might define the dynamic motor field, or pattern of contraction and extension of the continuous slab of muscle of a swimming fish or eel, with analog waves of muscular contraction travelling continuously from head toward tail, or in static form, the posture of an elephant trunk, swan neck, or snake body, that is held frozen in a sinusoidal or curved stance.

A variation on the analog wave function is the analog *magnitude* of the wave function,  $|u(x,y,z)|$ , shown in Figure 3.1 B, preserving its amplitude but discarding the polarity information. An approximation to this pattern can be observed in Falstad's Box Modes applet by setting the simulation speed so fast that the pattern flickers rapidly between green and red regions, creating the impression of

a three-dimensional pattern of yellow (red + green) lobes separated by dark nodes. This converts the red/green (alternating with green/red) polarized pattern of the first harmonic waveform, for example, to a twin-hump yellow/yellow pattern across the zero-amplitude node. This spatial pattern is also encoded in the standing wave signal where it is readily available for detection through a simple absolute value function.

The standing wave also encodes a stark binary pattern in the sign, or polarity of the standing wave pattern, that is,  $sign(u(x,y,z))$ , that evaluates to +1 where  $u(x,y,z)$  is positive, and -1 where it is negative, preserving the phase of the spatial pattern but ignoring its magnitude. This function can be approximated in Falstad's simulation by turning up the brightness control to maximum brightness, as shown in Figure 2.8 C. This is the kind of signal that would be used to define patterns like the sharply delineated black and white stripes of a zebra, and in motor control, this corresponds to the abrupt all-or-nothing type of motion seen in the jerky robotic bobbing motions of a walking bird, or the jerky movements of our eyeballs as they dart rapidly between fixations with abrupt starts and stops. This aspect of the spatial pattern is also readily readable from the standing wave with the use of a simple polarity or threshold function.

Finally, the standing wave also encodes a fourth pattern, that is the pattern of *nodes* of the standing wave, that is, the lines, surfaces, or vertices across which the polarity of the wave reverses, as shown by the gray planes in Figure 2.8 D. The nodal pattern is like an outline drawing that uses thin lines to depict the abrupt transitions between uniform patches of color in a cartoon. The pattern of nodal surfaces can also be seen as the *eigenfunctions* of the pattern, the centers of symmetry about which the pattern of positive and negative volumes alternates, the only regions that do not themselves alternate in polarity. The significance of this nodal representation of pattern will become clear in later chapters. All four of these patterns are encoded implicitly by the standing wave, where they can be read out locally at any point in the volume by simple local detectors that can be replicated throughout the volume of the resonating system, like the units that translate the chemical standing wave in morphogenesis to patterns of colors in animal skin, or to volumetric patterns of specific tissue types in the developing embryo, and like the cells of the cardiac muscle, or the cilia of a paramecium, that transduce patterns of electrochemical oscillations into mechanical contractions.

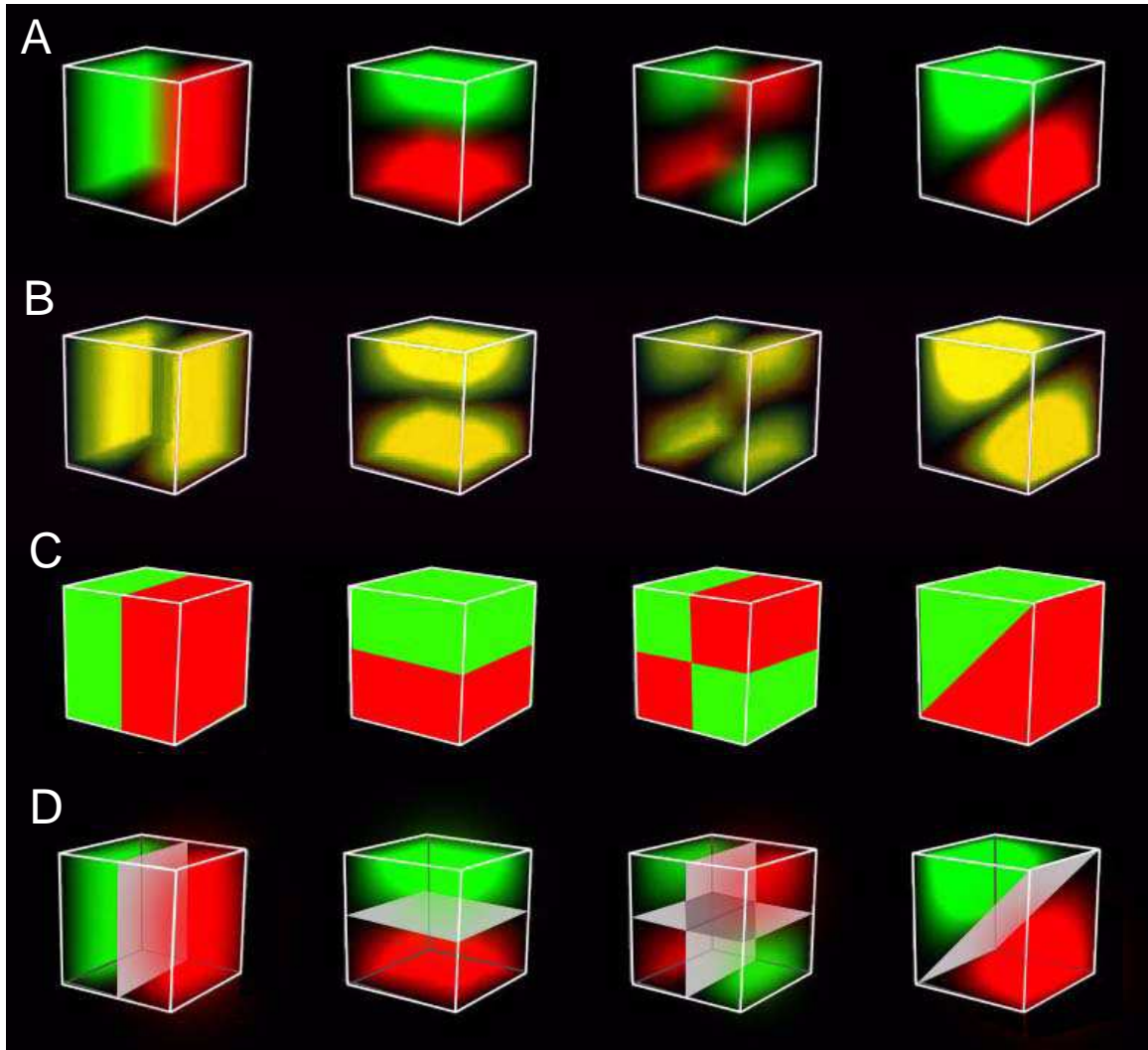


Figure 3.1. Four kinds of spatial information are present in the standing wave, which can be read out by simple local sensors distributed throughout the volume of the representation. A: An analog magnitude and phase. B: The absolute value of the magnitude, discarding phase. C: A binary polarity signal that discards magnitude but preserves phase. D: Nodal planes within which the vibration of the standing wave is zero.

### Sync Pulse to Read Alternating Signal

The standing wave pattern is actually in continuous oscillation, reversing polarity with every cycle. A simple local detector somewhere in the volume of the resonator would thus record an oscillating signal rather than a static pattern. In order to read out the static pattern represented by the standing wave, the detector must operate in phase with the oscillating signal so as to read it only in one phase of the cycle and not the other. This principle is demonstrated for example in the photographs of Murray's vibrating steel plates, shown in Figure 1.8. The patterns of light and dark shades in that figure were obtained by constructive and destructive interference between the light illuminating the vibrating steel plate, and that reflected back from the plate, which in turn depends on the instantaneous

pattern of deflection of the plate as it vibrates. Simple viewing with the naked eye or a simple camera would reveal no pattern at all, due to the rapid reversals of the light and dark regions of the pattern many times each second. In order to capture only one phase of the pattern and not the other, as seen in the figure, it is necessary to either snap the picture in a fraction of a second at the peak of the oscillation, or, to open and close the shutter in synch with the oscillation of the pattern in order to integrate light during one half-phase only. More generally, the standing wave pattern can be read out from a harmonic resonance representation by local detectors that detect periodically in phase with the oscillation. In other words, each simple detector distributed throughout the volume of the resonance representation must have access to two signals: the local oscillating standing wave signal itself whose waveform represents the signal, and a universal synchronization signal, or strobe pulse, that acts as a "read enable" signal, to turn on all the detectors in the volume only when the strobe pulse is in positive phase. The output of this conjunction, or logical AND between signal and strobe, defines an enduring static signal of volumes of positive and negative magnitude, distributed throughout the volume of the resonator as a wave function. While the standing wave pattern itself varies across the volume of the representation, the strobe signal is global, turning all the sensors in the volume of the representation on and off simultaneously in synchrony.

To take a concrete example in order to sharpen our mental image of this principle, imagine an array of tiny microphones suspended on an array of fine wires that form a 3-D lattice throughout the volume of the acoustical box described above, as suggested in Figure 3.2 A, in a way that does not interfere too much with the acoustics of the box. Each microphone records the local oscillations of air pressure at that point in the volume, and transduces it to an alternating electrical voltage that drives a simple circuit, as depicted in Figure 3.2 B, creating a current that flows clockwise around the circuit during the positive phase of the acoustical oscillation, and counter-clockwise during the negative phase. Two side loops connected to this circuit are equipped with light-emitting diodes (LEDs). Besides emitting light, the LED is also a *diode*, that is, a one-way valve that allows current to flow in one direction but not the other, like a check valve in a hydraulic or pneumatic system, or a ratchet in a mechanical system. In this circuit the two LEDs are biased in opposite directions, so that one side-loop allows current to flow only during the clockwise phase of the current, the other only during the counter-clockwise phase. Let us say that the clockwise current LED is green, and the counter-clockwise one is red. An acoustical standing wave vibration of say 30

Hz, picked up by the microphone, would thus cause the green LED to flicker at 30 Hz in synch with the positive phase of the wave, while the red LED would flicker at 30 Hz in counterphase to the green one during the negative phase. The rapid alternation of red and green would create an impression of yellow (red + green in additive color mixing) as shown in Figure 3.1 B. If the volume of the box were filled uniformly with hundreds of tiny LED circuits of this sort, then an acoustical standing wave in the box would manifest itself by a glowing field of LEDs everywhere throughout the box as a function of vibrational amplitude, leaving dark regions only at the nodes of the vibration where the acoustical vibration is zero. In other words, this circuit reveals the magnitude function  $|u(x,y,z)|$  of the standing wave.

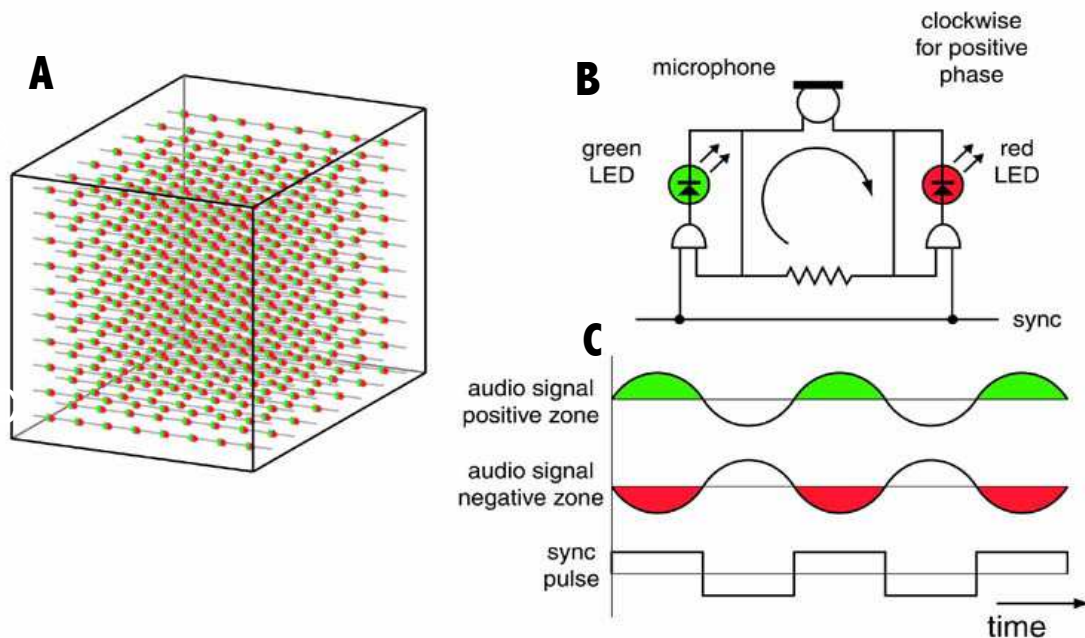


Figure 3.2. A: grid of tiny electrical circuits strung on an array of fine wires throughout the acoustical box, each consisting of B: a tiny microphone and two LEDs, wired so that the green LED lights up in the positive phase (clockwise current), the red one lights up in the negative phase. C: A sync pulse or strobe signal oscillating in phase with the standing wave serves as a “read enable” line to integrate only during the positive phase, turning on the green LEDs in positive zones, and red LEDs in negative zones of the standing wave.

Now to introduce a common strobe signal, let us say that the grid of wires on which the LED circuits are suspended is connected to a sync pulse that feeds all the circuits simultaneously with the same alternating sync signal, and this sync pulse is connected to the side-loop circuits by AND gates, that allow the side-loop current to flow only during the positive phase of the sync pulse, but blocks the flow during the negative phase, as shown in the circuit diagram in Figure 3.2 B. If the sync pulse is now alternated at the same 30 Hz as the acoustical standing wave, as suggested in Figure 3.2 C, it will turn on the green LED circuits during the

positive phase of the oscillation in the positive zones of the standing wave pattern, but shut off the red LED circuits during the negative half-cycle, resulting in a static or flickering pattern of green lights only in the green zones of Figure 3.1 A, whereas in the negative zones of the standing wave the sync pulse will turn on only the red LEDs during the positive phase of the sync pulse, and thus this simple local circuit replicated throughout the volume of the resonator will serve to light up the wave function  $u(x,y,z)$  as volumes of glowing green and red, as shown in Falstad's box modes applet. If the sync pulse is phase-shifted to be positive during the *negative* phase of the standing wave, this will reverse the patterns of red and green volumes to paint the negative lobes green and the positive lobes red, and shifting the phase to intermediate values will reveal a phase-shifted pattern of red and green zones.

The sync pulse can also be used to pick out or tune for particular components of an oscillating signal. For example given a compound standing wave composed of a fundamental oscillation along with one or more higher harmonics, when probed with a sync pulse at the fundamental frequency, would reveal only the fundamental component of the oscillation, not its higher harmonics, whereas when tuned to the frequency of one of the higher harmonics it would pick out the waveform of that harmonic component alone. The sync pulse can thus be tuned somewhat like a radio receiver to pick out the component or components of interest. This principle of tuning for features by oscillation frequency is also observed in the interactions between harmonics components of different frequencies in a compound oscillation.

### **Static and Dynamic Representation of Space and Time**

One of the most powerful features of a harmonic resonance representation is that the representation of spatial patterns by a standing wave automatically and inevitably also includes a representation of spatiotemporal patterns that are cyclical over time, achieved by oscillations out of synch with the fundamental resonance. Let us investigate this dynamic aspect of a harmonic resonance representation using Falstad's Box Modes applet again. The reader is encouraged to run the applet and follow along with the examples described below.

We begin with a first harmonic oscillation in  $x$ , by clicking the box [1,0,0] in the applet. This produces an alternating red/green green/red pattern that represents a single static waveform that alternates across a fixed static node plane. Clicking box [2,0,0] produces a second harmonic red/green/red pattern alternating with green/red/green, again, alternating across (this time) two static node planes, and

oscillating at a higher frequency. If you turn on both  $[1,0,0]$  and  $[2,0,0]$  at the same time however, as shown in Figure 3.3 A, then something strange occurs, due to the different temporal frequencies of the two components. The observed pattern alternates between green/red/dark, red/green/red, dark/red/green, as suggested in Figure 3.3 A through C, and then back again in reverse order, as suggested in Figure 3.3 C through A. There is a discrete, or stepwise character to this motion, as the waveform hops abruptly from one mode to the next.

To understand the meaning of this pattern of oscillation, now turn on all of the higher harmonics of this same series, that is, click on the squares  $[1,0,0]$  through  $[7,0,0]$ , as shown in Figure 3.3 D. These nodes represent frequencies that are 2, 4, 8, 16, 32, and 64 times that of the fundamental, or a series of octaves of the fundamental. The dynamic pattern now begins with a plane of positive green within the  $y/z$  plane, that sweeps progressively from left to right along the  $x$  dimension, as in Figure 3.3 D, E, and F, and when it reaches the end, it reverses direction and proceeds back from right to left again, as suggested in Figure 3.3 F, E, and D. This is a highly structured and orderly pattern of behavior across space and time, a reciprocal sweeping back and forth of a positive plane through an otherwise negative volume, and the sweep occurs in a series of eight discrete steps or jumps, rather than a continuous motion, and those discrete jumps can also be seen as ghostly “echos” of the plane at discrete intervals across the negative zones in Figure 3.3 D, E, and F. If you click off the higher harmonics of this resonance, i.e. shut off first  $[7,0,0]$  then  $[6,0,0]$  etc., you will see a progressive reduction in the number of steps in the motion, and at the same time a reduction in spatial resolution, that is, the plane of positive value becomes progressively thicker, so as to span the same volume in fewer steps. Conversely, adding higher harmonics increases the spatial and temporal resolution, producing (in the limit) a perfectly continuous sweep of an infinitely thin plane. What we have here is an explicit, extended spatiotemporal pattern that is reified across space and time, represented by a static combination of harmonic frequencies, and the spatial and temporal resolution are simultaneously altered by the addition or removal of higher harmonics. This is exactly the kind of pattern that would serve as a spatiotemporal pattern primitive, the dynamic equivalent of the static waveform functions in Figure 2.5 that serve as a basis set for static patterns. For example this kind of resonance could serve top-down as a motor control signal to produce coherent waves of contraction in a slab of skeletal muscle, or peristaltic contractions along a length of digestive tract, or synchronized waves of moving cilia on the surface of a simple creature, and the same principle could serve bottom-up as a sensory

function to detect waves of sensory stimuli in those same patterns, that is, an oscillating bar of light in a visual stimulus, or oscillating tactile sensation in a somatosensory stimulus, where the dynamic sensory stimulus lights up a static pattern of nodes whose phase differences represent that dynamic pattern.

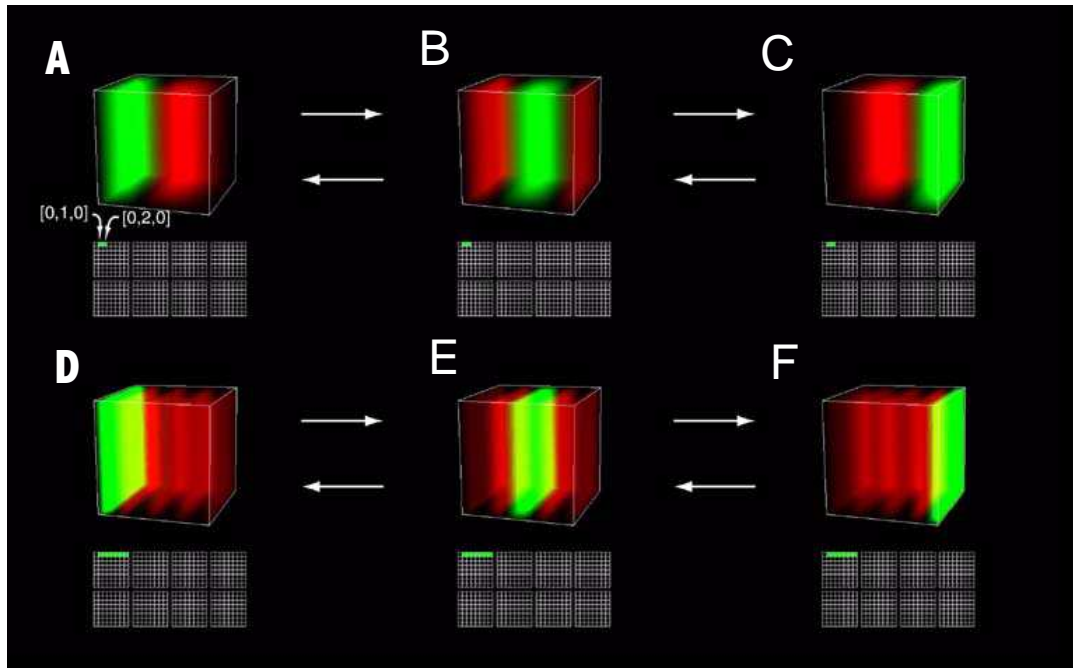


Figure 3.3. A: Turning on the first and second harmonics in  $x$  produces B: a green slab on the left, with red elsewhere, that moves in three discrete steps to the right, then back again to the left. C: Turning on the higher harmonics of this same pattern produces D: a thin slab of green, with red elsewhere, that also sweeps alternately left and but this time in eight discrete steps, a remarkably structured or ordered pattern of regular reciprocating motion.

Now let us try a different combination of harmonics, turning on the boxes  $[1,0,0]$  and  $[3,0,0]$  simultaneously, as suggested in Figure 3.4 A through C. This produces an interesting variation on the dynamic pattern above. This time a pair of red and green planes appear on opposite sides of a central node plane, and each plane oscillates back and forth across one half of the cube in mirror symmetry with the other, like two hands clapping, both reversing polarity as they meet at the center. In other words, the pattern goes through the sequence of Figure 3.4 A, B, and C, then it continues through two more stages, (not shown) that we could call D and E, which are mirror-reversed replicas of patterns C and B; then the sequence reverses again through E, D, C, B, and back to A again, and the whole forward and reverse cycle repeats indefinitely. Again, addition of higher harmonics in the same pattern, as shown in Figure 3.4 F through H, (and two more stages I and J, not shown) increases the resolution of this dynamic pattern across both space and time, while preserving the same basic pattern. With the addition of the

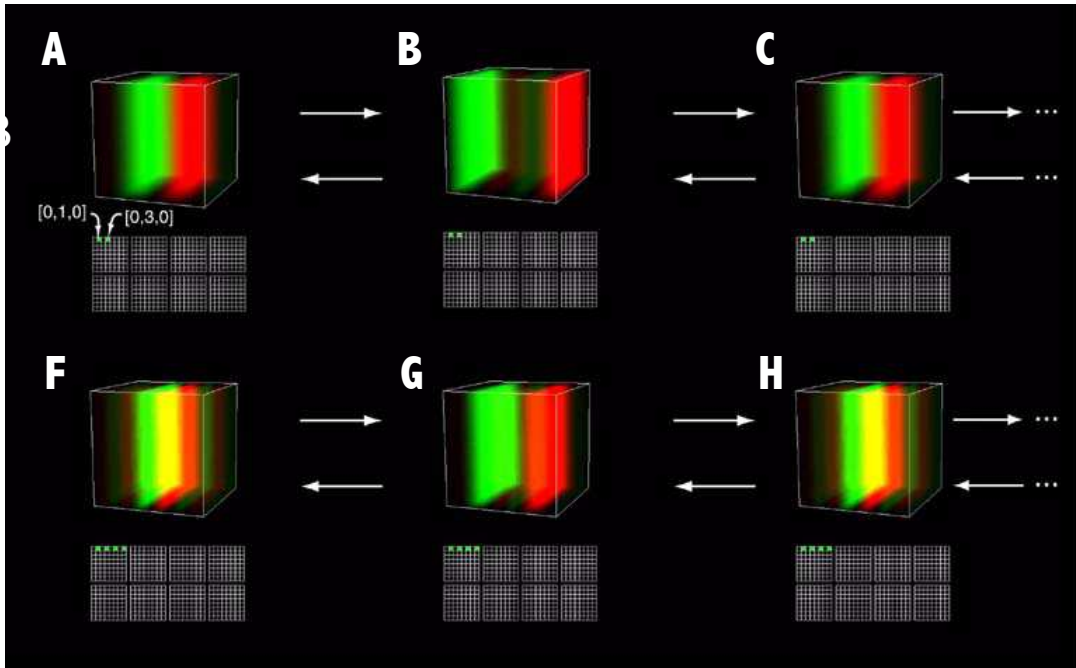


Figure 3.4. Turning on the first and third harmonics in  $x$  produces A: a pattern of green and red planes at the center, that jump B: left and right out to the ends, and C: back to the center, where they reverse color, and jump to the ends, then back to the center again (not shown) in endlessly repeating cycles. C: Adding also the higher odd harmonics (fifth and seventh) produces D through F: a refined version of the same inward and outward pattern, this time sweeping almost continuously in four little jumps out to the ends and back again.

higher harmonics, the pattern increases in resolution both in space and time, that is, the positive and negative planes get thinner, and the transition between F and G occurs in four discrete steps, instead of just two, as in A and B.

These same patterns of simple motion can of course be replicated in the  $y$  and  $z$  dimensions by the same principle, as the reader can easily verify with Falstad's simulation. Even more interesting is to observe the combinatorial patterns that emerge with simultaneous patterns in two dimensions. For example turning on the harmonics  $[1,0,0]$  through  $[7,0,0]$  at the same time as  $[0,1,0]$  through  $[0,7,0]$  creates two planes at right angles to each other, sweeping back and forth across the  $x$  and  $y$  dimensions simultaneously, and adding nodes  $[0,0,1]$  through  $[0,0,7]$  creates three sweeps at right angles to each other, an extraordinarily orderly and systematic pattern to emerge from such a simple resonating system. (Note: Falstad's simulation is arbitrarily limited to 10 harmonics presented simultaneously, so only lower resolution approximations to these patterns can be actually achieved in the simulation, although this limitation does not apply to a real resonance mechanism).

An even more intriguing pattern is obtained by the cross-product combination of harmonics across  $x$  and  $y$ , that is, by turning on nodes  $[1,1,0]$ ,  $[2,2,0]$ ,  $[3,3,0]$  ... up to  $[7,7,0]$ , as shown in Figure 3.5. This produces a peculiar compound sweep

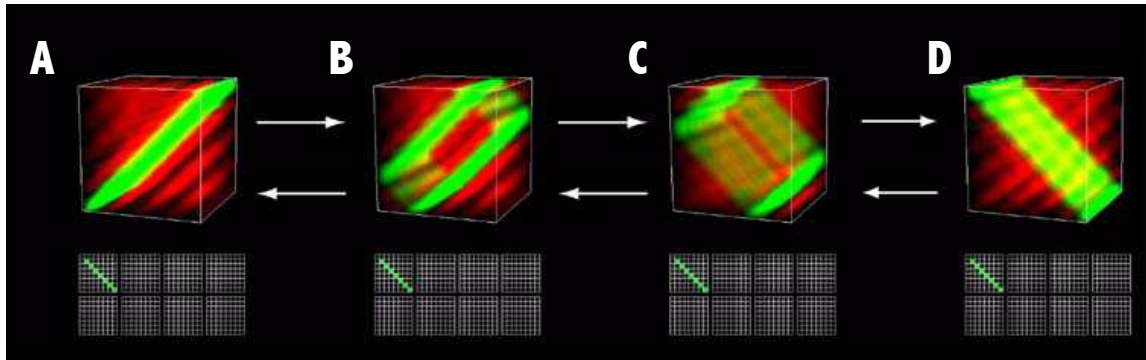


Figure 3.5. A: Turning on the  $[x,y]$  cross-product harmonics produces B: a diagonal green plane that expands outward like a hollow box then collapses back to a diagonal in the other direction, before reversing the sequence and returning to the initial configuration, and then repeating endlessly.

pattern that begins with a green plane of positive values in the diagonal  $x = y$  plane, as in Figure 3.5 A, that splits into two parallel planes connected on two sides like an open-ended box, as in Figure 3.5 B, that expands outward in opposite directions as a hollow box whose short sides grow as its long sides shrink, as in Figure 3.5 B and C, ending in a diagonal plane in the opposite direction (in the  $y = 1-x$  plane, shown in Figure 3.5 D) and then the pattern turns around and repeats in reverse sequence from D back to A, and the alternately reversing sequence continues in cyclic oscillation. Another extraordinarily complex and lawful emergent pattern from very simple parallel resonance principles, a two-dimensional generalization of the one-dimensional reciprocating sweep of the last example.

Finally, a still more interesting pattern is obtained by the full cross-product terms across  $x$ ,  $y$ , and  $z$ , that is, by turning on nodes  $[1,1,1]$ ,  $[2,2,2]$ ,  $[3,3,3]$  ... up to  $[7,7,7]$ , as shown in Figure Figure 3.6 A through D. This produces a strikingly intricate pattern of orthogonal sweeps back and forth between oppositely-oriented tetrahedra that span the opposite corners of the cube. The bright triangle in Figure 3.6 A is the near face of a tetrahedron, with corners at points  $\{0,0,0\}$ ,  $\{1,0,1\}$ ,  $\{0,1,1\}$  expressed in unit cube coordinates of the spatial domain, with the opposite vertex of the tetrahedron located at  $\{0,0,1\}$ , seen transparently through the triangular front face. (Note: *{curly braces}* are used to indicate coordinates in the *spatial* domain of the standing wave resonance in the box, while *[square brackets]* indicate harmonics in the *frequency* domain in the grid of little squares.) Each of the four triangular surfaces of the tetrahedron exhibits a bright green (positive)

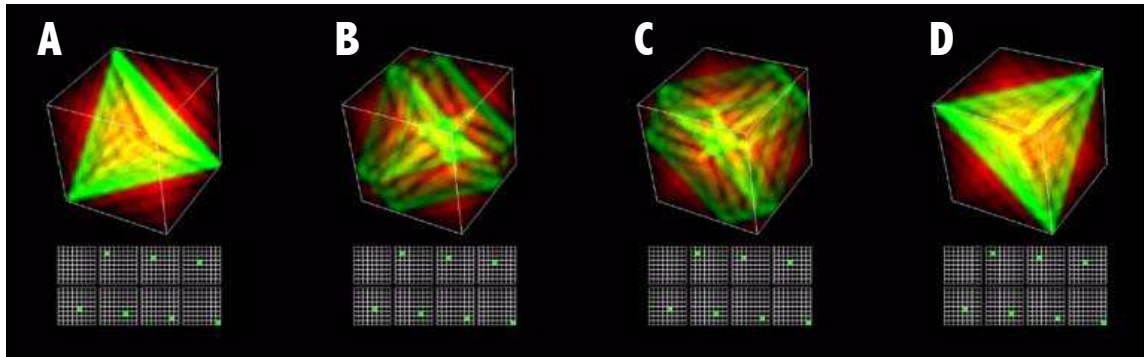


Figure 3.6. Turning on the  $[x,y,z]$  cross-product harmonics produces at first A: a tetrahedron. All four faces sweep toward their opposite vertices simultaneously, (B through D) crossing and reversing in the middle, producing a tetrahedron the other way, (D), with faces and vertices reversed, after which the pattern evolves back again in reverse sequence from D through C, B, back to A again, and so on in endless succession.

value throughout its surface, with red (negative) elsewhere, both inside and outside the tetrahedron. The four surfaces sweep simultaneously in a direction normal to their planar surface toward the opposite vertex, as shown in Figure 3.6 B through D, in a three-dimensional generalization of the growing/shrinking box of Figure 3.5, with an additional third dimension of symmetry in space and time. The final shape in Figure 3.6 D is inverted relative to the initial tetrahedron, with vertices now spanning the cardinal corners of the unit cube, that is,  $\{1,0,0\}$ ,  $\{0,1,0\}$ ,  $\{1,1,1\}$  and  $\{0,0,1\}$ .

The nature of this pattern can be analyzed by turning on its first component all by itself, that is, by clicking the node  $[1,1,1]$  alone. This marks the *cardinal* corners of the *spatial* cube in the resonance representation with positive polarity, that is, corners  $\{1,0,0\}$ ,  $\{0,1,0\}$ ,  $\{0,0,1\}$  appear green, while marking the opposite, complementary, or alternate corners as negative, that is, corners  $\{0,1,1\}$ ,  $\{1,0,1\}$ ,  $\{1,1,0\}$  appear red. If you allow the simulation to run, you will see these opposite corners alternate in polarity, the positive corners turning negative, and vice-versa;. Now turn on the next harmonic in the frequency representation, that is, click box  $[2,2,2]$  along with  $[1,1,1]$ . This serves to connect the positive corners with each other to form a fuzzy tetrahedron with unit-vector corners  $\{1,0,0\}$ ,  $\{0,1,0\}$ ,  $\{0,0,1\}$ , and negative elsewhere. Clicking still higher order harmonics  $[3,3,3]$ ,  $[4,4,4]$ , etc. preserves the same tetrahedral shape, but refines its spatial resolution to a crisp geometrical form. Now if you allow the simulation to run, you will see each of the four sides of the tetrahedron sweeping as a plane travelling in the direction of its surface normal, shrinking to a point at the opposite vertex of the tetrahedron, from whence it sweeps back again from the apex back to the base, and back again in endless cycles, all four sweeps occurring across all four faces and their opposite

corners of the tetrahedron simultaneously, a remarkably beautiful and intricate pattern of mirror-symmetrical motions, whose complexity emerges spontaneously from a simple resonance in a box. In fact, this is just a generalization of the pattern of motion shown in Figure 3.5 into the third dimension.

### Combinations of Different Dimensions

Other intricate patterns can be obtained by combinations of harmonics in different dimensions. The second harmonic pattern obtained by clicking  $[2,0,0]$  for the  $x$  dimension, or  $[0,2,0]$  for the  $y$ , creates a red/green/red or green/red/green “sandwich” pattern in the corresponding dimension, as seen for the  $x$  dimension in Figure 3.7 A. If you click both  $[2,0,0]$  and  $[0,2,0]$  simultaneously, as shown in Figure 3.7 B, you get a combination pattern that is a central cylinder surrounded

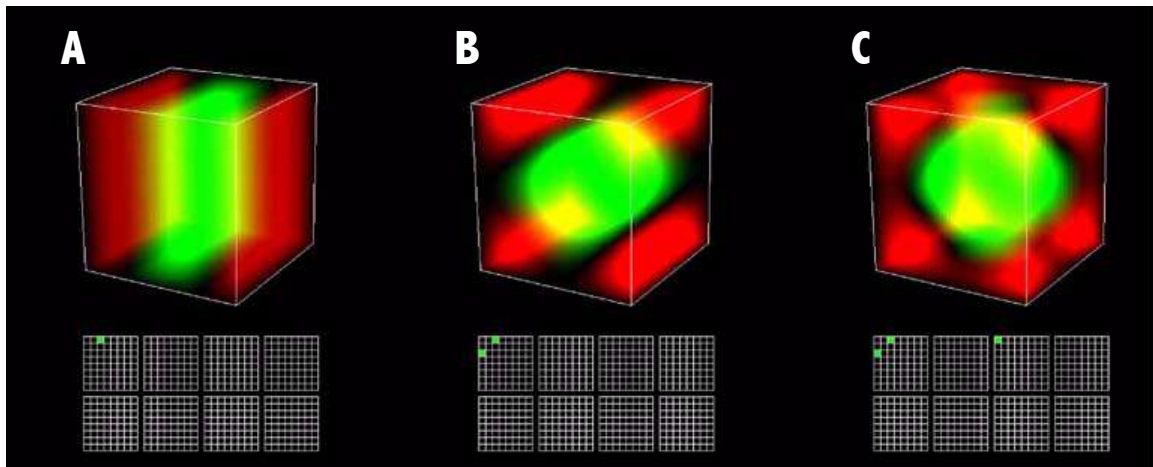


Figure 3.7. A: The second harmonic in  $x$  produces an on-center off-surround sandwich pattern. B: Adding the second harmonic in  $y$  produces a two-dimensional center/surround as a central green cylinder surrounded by red. C: Adding also the second harmonic in  $z$  produces a three-dimensional center-surround, a central green sphere encircled by a red surround.

by four corners of opposite polarity, as seen in Figure 3.7 B, a two-dimensional generalization of the center-surround contrast of the corresponding one-dimensional patterns. (Actually, the “cylinder” has a diamond-shaped cross-section rather than a circular one, as can be seen by increasing the brightness to approximate a polarity mapping of the pattern of  $\text{sign}(u(x,y,z))$ ) If you now click  $[0,0,2]$  along with  $[2,0,0]$  and  $[0,2,0]$ , as shown in Figure 3.7 C, you get a three-dimensional generalization of the center/surround concept that appears as a central sphere (actually an *octahedron*, or two pyramids attached base to base) surrounded by opposite-polarity corners. These spatial patterns are static, that is, the nodes remain fixed, although the positive and negative regions reverse alternately about those static nodes, because the  $x$ ,  $y$ , and  $z$  components oscillate at the same frequency.

## Rotation Through Relative Phase Adjustments

Falstad's Box Modes applet also allows you to change the relative phases of the component harmonics by dragging the mouse horizontally. This is exactly analogous to shifting the phase of the sync pulse as described above. When you click one of the little boxes in Falstad's simulation, it toggles the corresponding frequency node on or off with each click, with the phase set to zero, so when you click more than one box, they are automatically in phase with each other. But you can also click and drag the mouse horizontally in the little click box to shift the phase of the pattern from 0 to  $2\pi$ , which is indicated in the simulation by a tiny blue line that scans across the little click box like a tuner needle on a radio dial. For example if you click box [1,0,0] with the simulation stopped, to create a first harmonic green/red pattern, then drag the phase with the mouse, the waveform in the resonator will shift in phase with your mouse drag, which converts the green/red pattern to a red/green one, with a zero amplitude point in between the two opposite phases. With the simulation running, this has little practical effect on a single harmonic waveform when played by itself, but relative phase has a profound effect when the waveform is composed of two or more components.

(Falstad's Box Modes applet also allows you to adjust the *magnitude* of the wave by dragging the mouse vertically in the little boxes. This also has the effect of reversing the polarity of the waveform, because a magnitude of -1 swaps the positive and negative regions. We will be leaving the magnitude alone for the following demonstrations, and mention it here only to prevent confusion if this feature is encountered accidentally.)

Let us begin with a pattern of [1,0,0] and [0,1,0] simultaneously, as above, both clicked to phase zero. This produces a red/green pattern across a 45 degree angled nodal plane, as shown in Figure 3.8 A. Turning the individual components off and on again in turn, shows how the horizontal and vertical green/red patterns combine to create the diagonal one. Now click node [0,1,0] and drag it sideways to shift its phase. If the simulation is stopped, this will progressively change the angle of orientation of the node plane separating red and green regions, as shown in Figure 3.8 B, C, and D. If the simulation is running, however, it causes the entire pattern to rotate continuously, either clockwise or counter-clockwise, depending on the exact phase shift. As the phase shift is slowly increased from zero, the pattern rotates first counter-clockwise, and the rate of rotation rises to a peak at phase difference of 90 degrees, when the component waves are in *quadrature*, then reduces back to a stationary pattern as the phase difference passes

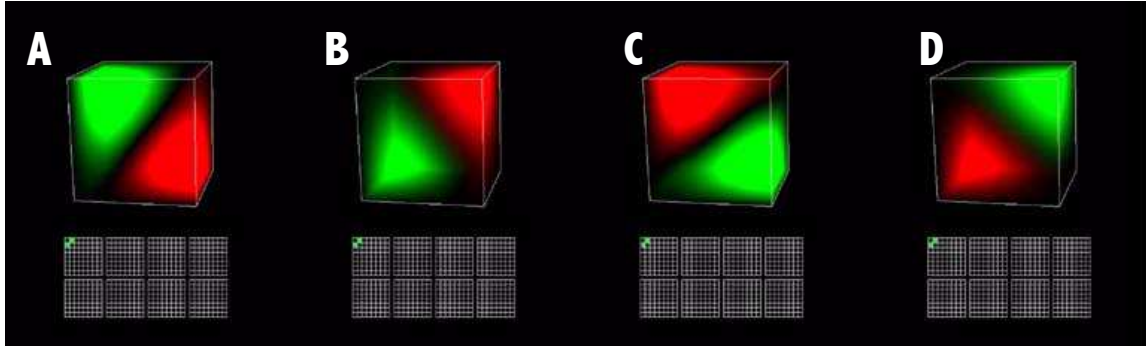


Figure 3.8 A: Turning on the first harmonic in x and y creates a green/red pattern oriented at 45 degrees. B through D: Advancing the phase of the y component sets the pattern into rotation at a rate that is proportional to the phase difference between the two oscillations, that reaches a maximum at quadrature (phase difference of 90 degrees), drops to zero at counterphase (180 degrees), then rotates in the opposite direction to a maximum at negative quadrature (270 degrees) and back to zero when back in phase.

through 180 degrees. If the phase is advanced still farther, the rotation begins again this time in the opposite direction, clockwise, as the phase of the y component is now retarded rather than advanced relative to the phase of the oscillation in x, reaching a maximum rotation rate when the waves are in negative quadrature. And if the phase is shifted still farther the phase shift returns to zero, and the rotation slows then stops. What we have here is a representation of a dynamic rotating pattern by way of a static phase relation between waveform components. Trigger two oscillations with the right frequency and phase relation, and you get a rotating pattern. This kind of dynamic pattern generation principle could be used for example in motor control, to produce a rotary pattern of muscular contraction, and in sensory systems, to capture or characterize the rotation of a dynamically cycling waveform pattern by the phase relation between its static harmonic components. In this example the rotation occurs through the x,y dimension. Clicking the z node [0,0,1] tilts the red/green divide 45 degrees in the x,z and y,z dimensions, and shifting its phase sets the pattern into rotation across the z dimension also.

Higher harmonics produce more complex spatial patterns, and phase shifting them produces more complex patterns of motion also. For the next example clear all active nodes, and click nodes [2,0,0] and [0,2,0] again, to produce the two-dimensional center-surround pattern in Figure 3.9 A, which is the same as Figure 3.7 B above. Now with the simulation stopped, progressively shift the phase of the y component [0,2,0] and you will see a progression of the pattern as shown in Figure 3.9 B through D. At first, the central green cylinder elongates vertically to an elliptical cross-section, as do the surrounding red zones, which link up vertically, as in Figure 3.9 B, and this pattern continues to morph into a simple red/

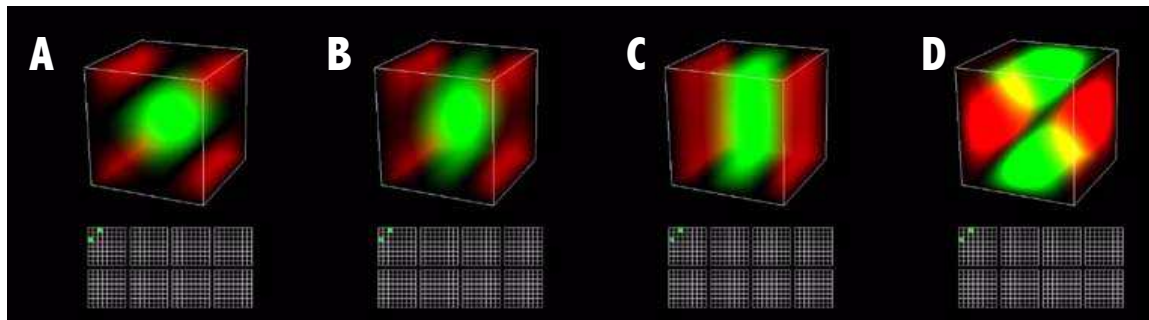


Figure 3.9. Starting with A: a second harmonic on-center off-surround in x and y, the phase of the y component is varied from B: a vertical elongation, to C: a center/surround in the x dimension only. Eventually the pattern shifts to D: positive lobes vertically and negative lobes horizontally. These are all spatial permutations and combinations of the on-center off-surround concept in different dimensions.

green/red sandwich of vertical slabs, as in Figure 3.9 C. This is the point where the phase of the y component is just reversing polarity, and thus the pattern is determined entirely by the x component alone, as can be easily verified by clicking the x node  $[2,0,0]$  off momentarily, and seeing pattern disappear altogether. Shifting the phase further still produces the pattern in Figure 3.9 D, with two red lobes left and right, and two green lobes top and bottom. Each of these phase shifts of the static waveforms produce their own characteristic combination pattern. But every combination also has a unique spatiotemporal pattern of cyclic evolution.

With the simulation stopped, re-adjust the phase of the y component,  $[0,2,0]$  until you get the central cylinder pattern in Figure 3.9 A. If you allow the simulation to run, the pattern alternates with its inverse across a static pattern of nodal planes. Now shift the phase of y a little farther again to get the elliptical cross-section stretched cylinder, and let the simulation run. Now we have a strange circulatory motion where pairs of blobs from left and right merge horizontally into a single blob at the center, which then splits vertically to a pair of blobs one above, one below, that move up and down respectively, away from the center, to be replaced by the next pair of blobs coming in from left and right to merge at the center, and so on round and round, joining horizontal, and splitting vertical in endless cycles. If you observe the behavior of the nodal surfaces that separate red and green volumes, there are four axes of rotation about which four nodal planes rotate in synchrony. And if you shift the phase of y to appear as in Figure 3.9 D, and then let the simulation run, the pattern will once again alternate between opposite contrasts across static nodal surfaces. The points where the nodal pattern is static are the points where the x and y component oscillations are symmetrically balanced in phase, whereas a phase that is advanced or retarded creates rotation

either clockwise or counter-clockwise, respectively. The maximum rotation rate that can be achieved in this kind of representation is obtained with waves that are in perfect quadrature, that is, with a phase difference of  $\pi/2$  or 90 degrees, at which point the rotation rate of the combined x/y pattern is equal to one full circle for every cycle of oscillation of the second harmonic oscillation, which in turn is four times the frequency of the fundamental. With rotational velocity expressed by the amount of phase lag and lead between two waveforms, it is natural for the phase difference to increase to a maximum at quadrature, diminish to a minimum again in 180 degree counterphase, and then build up again to a maximum in the opposite direction at negative quadrature before diminishing to zero again in-phase.

Waveforms that are composed of different frequencies in different dimensions always produce dynamic patterns of motion. For example clicking nodes [1,0,0] and [0,2,0] creates an oscillating pattern that morphs cyclically between the first harmonic in x pattern, green/red (or its complement) horizontally, as in Figure 3.10 A, and the second harmonic y pattern, a vertical red/green/red sandwich pattern

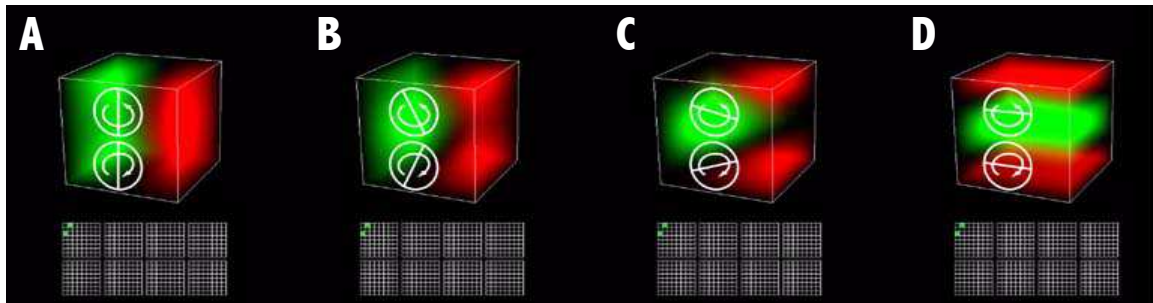


Figure 3.10. A first harmonic in x, along with a second harmonic in y, produces an oscillating pattern that begins as A: two parallel slabs, B: one bulges as the other shrinks back until C: the bulger cleaves the shinker in two pieces that move up and down respectively culminating in D: a second harmonic center/surround sandwich in y. The full cycle would continue four more frames to the right (not shown) in exact mirror symmetric pattern, ending with parallel slabs in the opposite polarity. It then reverses direction and cycles through all the same patterns in the reverse sequence, and then repeats indefinitely.

shown in Figure 3.10 D, passing through the intermediate stages in Figure 3.10 B and C, first left-to-right (A, B, C, D), then it continues through three more stages (not shown) which we could call E, F, and G, that are the exact mirror images of C, B, and A respectively, ending in a red/green pattern that is a mirror image of the green/red initial pattern, then the whole sequence plays back in the reverse direction again, G, F, E, D, C, B, A, and the cycle repeats alternately forward and backward in sequence indefinitely. This pattern of motion is best understood by observing the nodal planes that separate the red and green volumes, as suggested in the overlay. The nodal plane begins as a vertical surface between

red and green (A), then folds in the middle about a horizontal axis (B), the upper half rotating counter-clockwise, the lower half clockwise, as indicated by the arrows. As the rotation continues (C), the nodal planes become parallel (D), and the rotation continues through a full 360 degrees above and below, through E, F, and G (not shown), then a full 360 degrees back the other way through G, F, E, D, C, B, and A, totally inverting the volumes of red and green that they separate. In other words, this pattern represents symmetrically opposed rotations around two vortices in reciprocating alternation.

In this experiment there was no component in the  $z$  dimension, and thus the pattern is constant or unchanging with differences in depth, a straight projection of the 2-D pattern across  $x$  and  $y$  through the  $z$  dimension. We can describe the progression of patterns in Figure 3.10 A through D as a green and red slab; the green slab folds into a wedge, while the red slab splits into an anti-wedge, filling the space not occupied by the wedge; the angled surfaces of the wedge rotate to a parallel sandwich configuration as shown in D and beyond. We can now modulate the  $z$  dimension to generalize this pattern to a full three-dimensional shape. If we click on  $[0,0,1]$  along with  $[2,0,0]$  and  $[0,2,0]$ , this first harmonic in  $z$  is of the same frequency as the first harmonic in  $x$ , and thus oscillates in phase with it, rotating the pattern of reciprocating wedge and anti-wedge to run from one corner of the cube to the opposite, across the diagonal. If you click and drag the phase of the  $z$  component, the reciprocating wedge pattern begins to rotate in the  $x/z$  dimension, to appear just like the simple rotation in Figure 3.8 when viewed from the top, while still appearing as a reciprocating wedge and anti-wedge in the  $x/y$  dimension like Figure 3.10 when viewed from the front.

Now click off the  $[0,0,1]$  node and replace it with the  $[0,0,2]$  node, second harmonic in  $z$ , along with  $[1,0,0]$  and  $[0,2,0]$ . This second harmonic in  $z$  oscillates in phase with the second harmonic in  $y$ , which converts the wedge and anti-wedge pattern into its three-dimensional generalization, a cone and anti-cone in the  $y/z$  dimensions as shown in Figure 3.11 B and C. As in its two-dimensional projected wedge form, this pattern morphs continuously from two parallel slabs in Figure 3.11 A, to a cone and anti-cone in Figure 2-18 B and C, to a cylinder and anti-cylinder in Figure 2-18 D, then on to another cone facing the other way, (E and F, not shown) to parallel slabs in opposite polarity (G, not shown in the figure) and back again through the reverse sequence again, and on to endless sequential alternation. The rotation of nodal surfaces we saw in Figure 2-17 is now no longer a simple rotation about two axes parallel to the  $z$  dimension, but a higher order

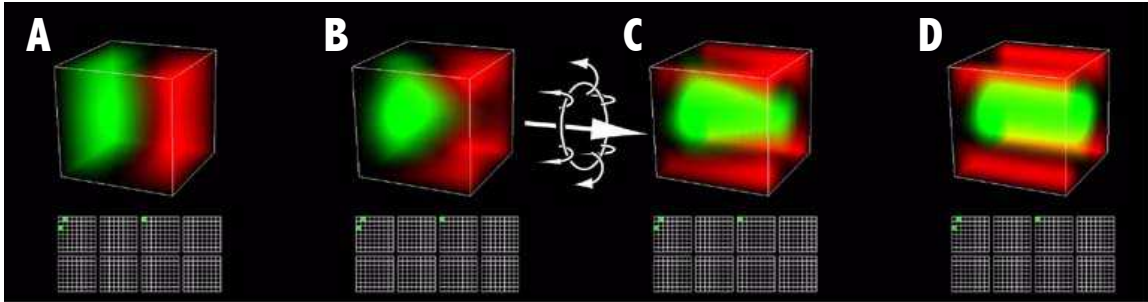


Figure 3.11. A: two parallel slabs, B: one bulges as the other shrinks back until C: the bulger punctures the shinker and D: turns into a positive cylinder surrounded by negative field. The full pattern continues through three more stages in exact mirror symmetry to the first four, ending with parallel slabs in the opposite polarity. It then reverses direction and cycles through all the same patterns in exactly the reverse sequence each cycle, and repeats again for ever and ever.

rotation about a circular axis of rotation embedded in the z/y plane, as suggested in the overlay, with rotation first left-to-right through the center of the circle (the advance of the puncturing cone) with a reverse counterflow right-to-left around the outside of the circle (the counter-movement of the anti-cone) as suggested by the overlay, and a reverse flow in the second half-cycle to the left at the center, and to the right in the periphery (not shown). This pattern is suggestive of the most primal reciprocating motions of coitus, a motor pattern observed even in some of the simplest organisms.

We could go on endlessly with more examples of spatial, or spatiotemporal patterns and the harmonics required to generate them. But the significance of this concept is not so much in the details of the representation, or exactly how it breaks down shapes to express them in a sinusoidal basis set, but the true significance of harmonic resonance is that it demonstrates how an explicit, spatially-extended volumetric representation can be coupled to an abstract featural mechanism that is capable of both detecting patterns present in the representation bottom-up, as in visual recognition, as well as projecting patterns into the representation by reification, or filling-in, demonstrating the constructive, or generative perceptual function that is clearly a significant aspect of perception, and yet prominently absent from most models of perceptual representation and processing. And this explicit spatial representation is expressed in a holistic Gestalt-like mechanism that captures some of the observed field-like aspects of perception and conscious experience.

### **The effect of Resonator Shape**

Although the cubical box of Falstad's Box Modes applet exhibits an extraordinary repertoire of complex patterns and combinatorial patterns, all of these patterns are

related to the cubical form of the resonator itself. Even the complex tetrahedral patterns in Figure 3.6 are merely reflections of the cubical symmetry of the box, tracing the medial axis planes of symmetry between orthogonal faces of the cube. We see the same principle in the Chladni figures, that depend so much on shape of the resonating plate. Square plates produce rectangular and diagonal patterns and sub-patterns, circular plates create radial and concentric patterns, triangular plates produce symmetrical partitions of the triangular form, as seen in Figure 1.16. And so also in three dimensions: a spherical resonator creates concentric, radial, and lateral type subdivisions, as seen in the atomic orbitals of Figure 1.18, whereas the cubical box creates the patterns shown in Falstad's Box Modes applet. This strict dependence of the family of standing waves on the geometry of the resonator is useful for some applications, such as motor representations, where the shape of the resonator can be tuned to match the fixed topology of the body, but not so useful in others, as in perception, where the range of possible patterns or spatial interpretations of a stimulus should ideally remain as unrestricted and universal as possible. We will discuss later how this invariance aspect of perception can also be achieved in a harmonic resonance representation.

The usefulness of standing (and/or travelling) waves as a motor representation was discussed in chapter 1, with the example of a swimming eel, depicted in Figure 1.13, where the sinusoidal motor pattern propagating continuously from head towards tail, is modeled by a travelling wave in a cylindrical resonator, because a cylinder is a close enough model of the muscular topology of an eel. But where is this resonance located? Are we talking about a resonance in the eel's brain and spinal cord, which is transmitted to the muscles by motor neurons? Or are we talking about a resonance in the muscle tissue of the eel, waves of electrochemical polarization and depolarization that create waves of contraction and extension in bulk muscle tissue? The example of coordinated motor patterns in simple creatures lacking a central nervous system, and of the cardiac muscle that continues to pump even after the cardiac nerve has been severed, demonstrate that it is *possible* for coherent waves of muscular contraction to emerge spontaneously in the absence of stimulation from motor neurons and a central nervous system, and it is unlikely that this basic property was lost when the central nervous system first evolved. More likely, the central nervous system evolved so as to make use of this more primal basic principle of spatial representation already inherent in muscle tissue. The central nervous system spurs the muscles into activity like a cowboy spurring his horse to stimulate a

gallop, but the orderly waves of periodic contraction and extension that propagate through the muscles of the galloping horse are not sculpted or reified by that sparse and punctate stimulus, nor by the punctate motor neuron activation that the spurs indirectly trigger, but rather they emerge spontaneously from natural oscillations within the horse's brain, nervous systems, and musculature acting in unison, in response to the sparse stimulus.

This concept finally offers an explanation for the relatively sparse distribution of motor neuron synapses across muscle tissue, or *innervation ratio*, which can often be several thousands of muscle fibers for each motor neuron. According to the conventional explanation, each individual motor neuron innervates a patch of muscle tissue through a set of motor synapses distributed across the patch, to form a "motor unit", and patterns of motor contraction are explained by patterns of firing of such motor units triggered by activation in their motor neurons. According to this explanation, a patch of muscle in the motor unit integrates the activation from all the synapses in the patch, and contracts in proportion to a kind of average of all these scattered stimuli. This is basically a top-down concept, with all motor commands arriving top-down from the motor cortex. According to the resonance model on the other hand, the motor units do not form or define the waveform of muscular contraction, they merely trigger and synchronize it. But the contractile waveform itself emerges from the muscle tissue in response to stimulation, as a spatial reification process that occurs down in the lowest level within the muscle itself. This distinction could be tested neurophysiologically, at least in principle, by severing individual motor neurons in the middle of a muscle, and observing whether contractions stimulated in adjacent regions propagate also across the denervated region.

If the contractile motor pattern is indeed sculpted primarily by natural endogenous resonances, then the most effective way to trigger and modulate or control those resonances in the muscles would be with resonances in the motor system tuned to lock into and synchronize with the resonances in the muscles. In other words, the central nervous system also operates by harmonic resonance, that is, by coherent patterns of standing waves and travelling waves throughout the brain and nervous system, that communicate synchronous oscillations across widely separated locations. Perhaps the most powerful aspect of a harmonic resonance model of nervous system function is the natural tendency of resonating systems to couple with each other to establish a global resonance that is tuned not only to the natural resonances of its component parts, but also to the resonance of the

emergent whole created by the coupling of the individual parts, as we see in the coherent waving of cilia in the paramecium, and in the coupling of oscillators like adjacent pendulum clocks, and the synchronous oscillations across the molecules of a crystal oscillator. This is the *Gestalt* in Gestalt theory, the whole is more than the mere sum of its component parts. The natural unifying properties of harmonic resonance are responsible for the coherence and synchrony between the experience of colors, motions, and sounds in perception, the coherence and synchrony of body motions in locomotion, mating, and dance, and the coherence and synchrony of perceptual experience with motor function, as a dancer matches their movements to those they perceive in their dancing partner, or as musicians synchronize their playing motions to the sounds they are perceiving from the rest of the band. The powerful unifying and synchronizing force of harmonic resonance is ultimately responsible for unity of conscious experience.

### **Rotation Invariance in Perception**

The strict dependence of a harmonic resonance system on the geometry of the resonator is a disadvantage in the case of perceptual or cognitive representation, whose spatial patterns should ideally be determined by the properties of the stimulus, rather than of the resonator, so as to be able to represent any arbitrary shape that might be perceived, or imagined in mental imagery. It turns out that harmonic resonance has some pretty unique invariance properties that are extremely useful for a perceptual representation. In Figure 2.6 A we introduced the mechanism of a cubical box, with speakers mounted on three orthogonal faces, connected to three signal generators, that produce the x, y, and z components of the standing wave in the box. This mechanism does not have rotation invariance, because it draws a distinction for example between a second harmonic in x and a second harmonic in y, even though they are the same pattern only presented at a different orientation. The cubical “bottle” on the other hand, shown in Figure 2.6 B, and its related rank of organ pipes in Figure 2.6 C, is significantly different in this regard. Blowing air across the mouth of this cubical bottle is most likely to produce vertical pressure fluctuations, and thus standing waves in the y dimension, because the mouth of the bottle is located at the top of the box, so the pressure tends to fluctuate in and out of it. But it is in the nature of resonance that in fact any of the harmonics of the bottle can emerge, with greater or lesser probability, if sufficiently energized with a high velocity air flow, like the different harmonics of a bugle that can be obtained by pursing the lips and blowing harder. And among those many possible harmonics are the second harmonic in x, y, and z, any of which can appear in the bottle, especially when encouraged by

careful positioning of the air stream. And the vibrational frequency of each standing wave pattern depends on the pattern itself, not its orientation. Therefore the “detection” of the presence of this second harmonic pattern by a sympathetic resonance in the second harmonic organ pipe, is a detection that is invariant to the orientation of the wave, it is a rotation-invariant recognition of the standing wave pattern in the resonator, at least for the six canonical orientations of the cube.

A similar distinction holds for the microphone that is used to record or sample the standing wave, like the microphone in Figure 3.2 B. A simple diaphragm microphone records the transient pressure fluctuations across the opposite faces of its diaphragm. A standing wave in the  $x$  dimension creates pressure fluctuations only across the  $x$  direction, so a microphone diaphragm oriented parallel to the  $x,y$  or  $x,z$  planes, could not pick up the  $x$  component of the vibration at all, because pressure fluctuations on one side of the diaphragm are exactly balanced, or cancelled by identical fluctuations on the other side. A simple diaphragm microphone therefore is a directional detector. But the microphone can be easily modified to make it invariant to orientation by sealing the back side of the diaphragm in a housing that is connected either to an external pressure reference, or to a closed reservoir of compressible air, to provide a pressure reference independent of the fluctuating pressure at that point in the resonator. This kind of microphone is omni-directional, it will pick up acoustical vibrations across the  $x$ ,  $y$ , and  $z$  dimensions, and in fact, most microphones are baffled in exactly this manner for this reason.

The issue of directional invariance applies equally to loudspeakers. When the diaphragm of a simple loudspeaker advances (and retreats) during vibration, it creates a pulse of higher (lower) pressure in front of the diaphragm and lower (higher) pressure behind it, two complementary waves that cancel each other destructively around the edges of the speaker, leaving only a directional vibration in front of the diaphragm, and its negative mirror image behind it. As with the microphone, the speaker can be made omni-directional by sealing the back side of the diaphragm and connecting it to an independent external or internal reference, thus converting the alternating positive/negative pressure dipole of the directional speaker, to an effective “monopole” of alternating pressure at one location, that alternately injects and extracts pulses of air in the resonator, producing a spherically propagating wave from that source, expanding like rings in a pond. (The principal purpose of speaker boxes in audio systems is to seal off

and baffle the negative wave from the back of the diaphragm, to prevent destructive interference with the positive wave from the front, and that is why speakers sound much quieter when removed from their speaker boxes.) The distinction between directional and non-directional detection (through microphones) and emission (through loudspeakers) bears on our model of resonance in the acoustical box.

If the resonator box filled with an array of glowing LED circuits depicted in Figure 3.2 A, were constructed using directional microphones, there would have to be three orthogonally-oriented microphones, with three amplifier circuits, at every location in the grid, and the oscillations would occur entirely independently across  $x$ ,  $y$ , and  $z$  dimensions. But if the microphones are configured to record omnidirectionally, then they would detect sound waves in  $x$ ,  $y$ , and  $z$  dimensions, and thus only one circuit would be required at each location, and the response of the system would become invariant to the orientation of the pattern in detection. It is the same circuits that resonate, for example, to a second harmonic wave pattern, whether oriented in the  $x$ ,  $y$ , or  $z$  dimension. If an omni-directional resonator of this sort is connected to omni-directional detectors, like the organ pipes suggested in Figure 3.2 C, then the presence of a second harmonic of any orientation in the box would trigger a sympathetic resonance in the second harmonic organ pipe, and the resonance in the organ pipe would in turn amplify the corresponding waveform in the resonator.

### **Huygen's Principle and Phased Array Antennas**

A regular grid or lattice of identical loudspeakers, or other wave sources, can generate coherent globally patterned waveforms by Huygen's principle, as seen in phased array antennas. According to Huygen's principle, a wave front propagating through space is equivalent to a line of point sources, each propagating waves that radiate outward like the rings in a pond when a stone is thrown in. If a straight line of stones is dropped into a pond simultaneously, the outward-propagating rings from each individual source add together by constructive and destructive interference, summing together their common component, which is a wave front parallel to the line of sources propagating outward at right angles to the line, while all the other waves cancel each other by destructive interference. This too is a distinctly Gestalt phenomenon, where the global coherent configuration is preserved, while the local artifacts quickly fade due to lack of global support. This principle is employed in phased array antennas, where the phase of the signal in each individual antenna of the array is carefully tuned to produce the desired

global waveform. For example if the antennas in an array are triggered to emit a train of pulses in uniform sequence from left to right, this will produce a moving wave, travelling left to right, at a speed determined by the time interval between successive pulses, which will leave a pair of angled wave fronts in its wake, like the bow waves of a boat moving left to right. If the antennas are triggered in two waves, one travelling left-to-right, one right-to-left, to meet at the center, this will create two sets of angled waves, like the bow waves of two motor boats that collide head-on in the middle. And if the speed of the propagating wave is varied as a quadratic function of distance from the center, starting faster near the periphery and slowing to some speed at the center at the collision point, this can create parabolic waves propagating outward as if from a parabolic dish, all from a flat antenna. This is the principle employed in modern phased array radars, in which a flat antenna composed of a grid of identical transmitter elements, generates a focused radar beam as if projected from a parabolic antenna dish, and the direction of the projected beam can be controlled on the fly by varying the phase of the signals radiating from one side of the antenna relative to the other, creating a fully steerable focused beam from a fixed flat antenna with no moving parts. This same principle allows the array of omni-directional loudspeakers in our acoustical box to generate virtually any waveform travelling in virtually any direction, by simply controlling the relative phase of transmission from the individual speakers. The phased array principle also operates in reverse, for a receiver antenna instead of a transmitter, that allows a fixed flat antenna to receive as if it were a steerable parabolic antenna, by simply time-delaying the signals from the individual receptor elements by the same pattern as that used in transmission. For focused detection of a distant source that is radiating waves outward in expanding shells, it is necessary to time-delay the signals from the center of the antenna relative to those in the periphery, so as to receive the spherical wave fronts simultaneously from the periphery and the center, and at every intermediate point, each delayed by the appropriate quadratic function, as if the detectors were mounted on a parabolic surface instead of a flat one. The quadratic time delay turns the flat antenna into a functionally parabolic one, and further time-delaying the signals coherently from left to right, or top to bottom, makes the antenna functionally equivalent to a steerable radar dish.

The phase patterns required for a phased array radar are computed on the fly by on-board digital hardware following mathematical formulae. How could these kinds of computations be performed in the wetware of the brain, or in the case of a simple acoustical box? The answer is to make use of the principles of harmonic

resonance itself to perform the required computations to define coherent spatial patterns for a phased array transmission. A first harmonic standing wave, for example, vibrating in the acoustical box, creates a coherent wave front that travels back and forth in orderly fashion from one side of the box to the other, triggering the array of microphones arrayed within the box with exactly the right pattern of synchronized waveforms that correspond to the first harmonic resonance. For example if the audio signals from all of the microphones in the array throughout the box were recorded in a multi-track acoustical recording, then played back in the same box, with each track played back in the same location where it was recorded, this will re-create the original first harmonic standing wave back in the acoustical cavity. Furthermore, this re-creation is not just a top-down pattern imposed on the resonator, but rather, it is a re-creation of the original harmonic conditions that formed that first harmonic standing wave in the resonator in the first place. The wave emerges spontaneously in response to the trigger of the phased array pattern encoded in the loudspeaker signals. As in the case of the enervation ratio of the motor units described above, the phased array signal need not recreate the whole waveform in all its sinusoidal detail in a totally top-down process, it merely needs to trigger the emergence of a first harmonic resonance in the resonator, and this can be achieved even with a very sparse “enervation ratio” using only a handful of loudspeakers that capture a coarse sampling of the required waveform in the acoustical box, to recreate that wave back in the same box at the full original resolution. As that first harmonic emerges, it automatically sculpts itself to mathematical perfection by simple resonance in the resonator. All that is required of the “top-down” signal is to favor the first harmonic over other harmonic alternatives, the resonance itself will take care of filling-in or reifying the waveform to its maximal resolution.

This concept of phased array triggering of spatial standing waves offers a paradigm to explain the intimate coupling between spatial patterns in the different cortical and sub-cortical areas across the brain. For conceptual clarity, we have been discussing microphones and loudspeakers as distinct reception and emission devices. In fact, microphones and loudspeakers operate by exactly the same principle, a simple microphone will also serve as a loudspeaker, and vice-versa. For reciprocal coupling between cortical areas, it is more useful to think of the microphones and speakers in the acoustical box as one and the same element that can work in both directions, transducing vibrations of the diaphragm into electrical oscillations in a circuit, and transducing electrical oscillations in the circuit to vibrations of the diaphragm. Picture a pair of acoustical boxes, each

equipped with an array of microphone/speakers, with a set of parallel connecting wires that connect each mike/speaker in one box to the mike/speaker at the corresponding location in the other box. A standing wave stimulated in either box will tend to stimulate the same standing wave in the other box, the two boxes will resonate together in a larger coupled resonance of both boxes simultaneously, in which any modulation of the resonance in one box will be communicated immediately and in parallel to the other box. This, I propose, is the principle by which standing wave patterns in one cortical, or sub-cortical area are transmitted to adjacent areas, and also how the retinal image is transmitted up the optic nerve to the brain.

### **Full Rotation Invariance with Spherical Resonator**

The rotational invariance of the standing waves in a cubical box is a direct consequence of the number of rotational symmetries of the cube, that is, that the cube remains geometrically identical at six different orientations (12 different directions, if polarity is considered), and thus resonances at those orientations are essentially identical. An even more impressive degree of rotational invariance can be obtained by using a still more symmetrical resonator. If the cubical resonator is replaced with a spherical one, the family of standing wave patterns changes from the cubical repertoire to the spherical harmonic series, with its patterns of concentric shells, and periodic stripes like the lines of longitude and latitude on a globe. Any of these spatial patterns can appear in the resonator at any orientation, while vibrating at a frequency that is characteristic to that waveform whatever the orientation, and thus the spherical resonator offers a completely rotation-invariant representation.

Invariance in recognition implies a many-to-one relation between the basic pattern and its many possible manifestations. For example a spherical harmonic, such as the third harmonic of the d-mode resonance shown in Figure 3.12 A, can appear at a range of orientations in three dimensions, while being the same essential pattern. A bank of tuned resonators, like the rank of organ pipes depicted in Figure 3.12 B, would respond to this characteristic pattern independent of its orientation through a full 360 degree rotation in any of three dimensions. But what about the top-down influence? If the organ pipe corresponding to this third harmonic pattern is energized top-down before there is any discernable pattern in the resonator, as suggested in Figure 3.12 C, which orientation will the pattern choose to appear in the resonator? If the top-down resonance can create a standing wave at any orientation, how would it choose one orientation to reify over all the other

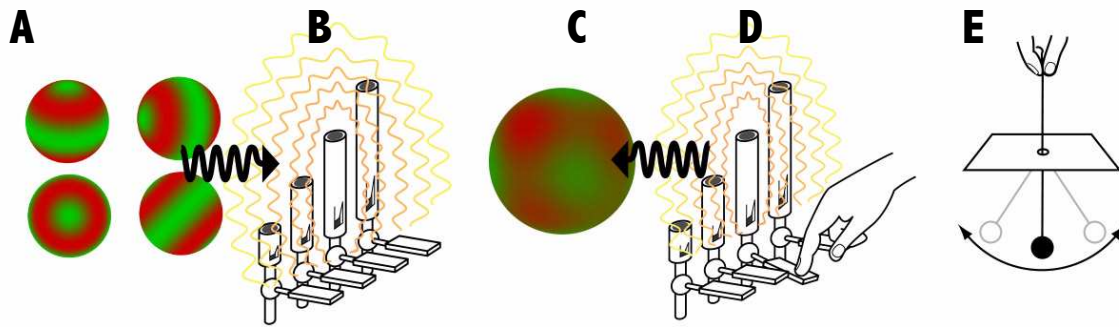


Figure 3.12. A: A third harmonic d-mode spherical harmonic resonance has a characteristic vibration frequency that is invariant to its orientation, and thus B: a bank of tuned resonators would serve as a rotation-invariant representation of that pattern. D: If that third harmonic is stimulated top-down, it will C: attempt to reify the corresponding standing wave pattern at all orientations simultaneously, producing an unstable indeterminate pattern, but if the priming is strong enough, it will select one orientation over the others, by the same principle that E: a pendulum's swinging can be amplified even if the orientation of its oscillations is unknown.

alternatives? The answer to this question turns out to involve one of the most interesting features of a resonance representation, the ability to perform top-down priming through an invariance relation. This principle will be explained with a simple analogy.

Imagine a pendulum on a string that is free to swing in both  $x$  and  $y$  dimensions, but whose support string passes through a small frictionless hole in a horizontal floor or divider between the pendulum bob and its point of support, as suggested in Figure 3.12 D. If the pendulum is set to swinging, the fact that it was swinging could be detected at the support point even if the bob could not be seen from above the floor, by a periodic variation of string tension due to centrifugal force as the pendulum swings, although it would be impossible to determine from above what direction the pendulum was swinging below the floor. The oscillating tension of the string can be seen as a rotation-invariant signal indicating the swinging of the pendulum at some orientation, independent of the orientation of that swinging. Is it possible to amplify this oscillation in the invariant representation above the dividing floor without knowing its orientation? How can the pendulum be given periodic pushes to keep it swinging in the direction it is already swinging, without knowing what that direction is? More generally, is it possible to provide top-down feedback and amplification across an invariance relation? In this case the answer is yes, by simple sympathetic resonance. If the pendulum is hanging motionless, it is impossible to pump it into swinging by gently pulling up and down vertically on the string's support point, the pendulum would simply remain vertical as it moves up and down. However if the pendulum already happens to be swinging even just a tiny bit in any direction, then synchronized pulling at the support point, timed to

coincide with the periods of increased string tension, will amplify the swinging of the pendulum at whatever orientation it happens to be occurring, without any knowledge above the horizontal floor as to which direction of oscillation is being amplified. In fact, even if the pendulum were initially motionless, *vigorous* up-and-down oscillation of the support point would inject random oscillations which could subsequently be amplified by further synchronized oscillation. This is the same principle by which an invariant higher-level representation can serve to amplify its pattern through an invariance relation, amplifying preferentially the one oscillation orientation that is already the most active, at the expense of all the alternatives.

This principle will apply in the condition shown in Figure 3.12 C. At first, playing the third harmonic note top-down in the absence of any coherent pattern in the resonator, will attempt to activate the third harmonic standing wave at all orientations simultaneously, as suggested in Figure 3.12 C. If the top-down priming is weak, the system will remain in this indeterminate state, with a third harmonic oscillation at many different orientations simultaneously, as a fuzzy superposition of states. But if the amplitude of the priming is increased sufficiently, the pattern at some random orientation will happen to be stronger than the others, and as this occurs, a positive feedback loop with the top-down resonator will preferentially amplify that one orientation over all the others, a top-down priming with reification across an invariance relation. Furthermore, after the top-down priming has established a reified manifestation of its corresponding third harmonic pattern in the resonator, that pattern will remain free to rotate to any other orientation as long as the priming continues, because its orientation is not constrained by the priming, but remains a free variable. This is a very significant feature of a harmonic resonance representation, inherited directly from the physical phenomenon of harmonic resonance itself, that captures an essential aspect of perceptual recognition and reification.

For example we can easily recognize simple geometrical shapes such as cubes, rectangular blocks, pyramids, tetrahedra, etc. independent of their orientation; our recognition of simple forms is rotation invariant. But although our recognition is rotation invariant, it is not at all “blind” to orientation; we can easily see the orientation of the recognized object as soon as we recognize its characteristic form. We both perceive it, and perceive it to be at a particular orientation. Furthermore, we can easily reify the hidden rear faces of the recognized object, predicting the exact location and orientation of its hidden faces and vertices based on its visible portions, and we can even recognize and perceptually complete by

reification objects which are partially occluded by foreground obstacles, even if the object is translating and rotating randomly through different orientations while we view it. This invariance in perceptual recognition, but *specificity* in perceptual reification, has been one of the most persistent unsolved riddles of perceptual function.

The principle of this invariance can be easily demonstrated using a Chladni plate. As in the case of a spherical resonator, a standing wave pattern on a circular Chladni plate can appear at any orientation, and each standing wave pattern will vibrate at its own characteristic frequency. An audio recording of this resonance, when played back in the presence of the circular plate, will tend to recreate the original standing wave pattern back on the plate, but the pattern can appear at any orientation. If the top-down priming is sufficiently strong, then one orientation will emerge as the dominant one, and amplify itself at the expense of the alternatives by positive feedback with the invariant resonance.

Rotation invariance is a very powerful feature of a harmonic resonance representation, as it helps to resolve the combinatorial explosion that would arise if every variation of the pattern (in this case every orientation) required a separate and distinct pattern template (in this case standing wave) to either detect or regenerate that pattern. Even more impressive invariances can be achieved by using a *gradient refractive index*.

### **Gradient Refractive Index**

Besides the geometrical shape of a resonator, another factor that influences the shapes of the standing waves in a resonator is the *gradient refractive index profile*, as it is called in optics, a coherent modulation of the speed of wave propagation through the medium to vary continuously as a gradient across the resonator. Falstad's Box Modes applet assumes a uniform speed of wave propagation, or speed of sound throughout the resonator, as is typical of an acoustical system. If the resonator is composed of biological tissue, however, this need not be the case; it is possible to create resonating systems in which the speed of wave propagation (or refractive index) varies significantly across the resonator, according to some regular function, as in the example of *gradient refractive index* (GRIN) optics. Figure 3.13 A shows a GRIN lens in the shape of a cylinder whose refractive index varies continuously as a function of radial distance from the cylindrical axis, with greater refractive index toward the center, indicated by the shading. Typically a parabolic or exponential gradient refractive index profile is used, as shown in Figure 3.13 B. This has the effect of bending light in

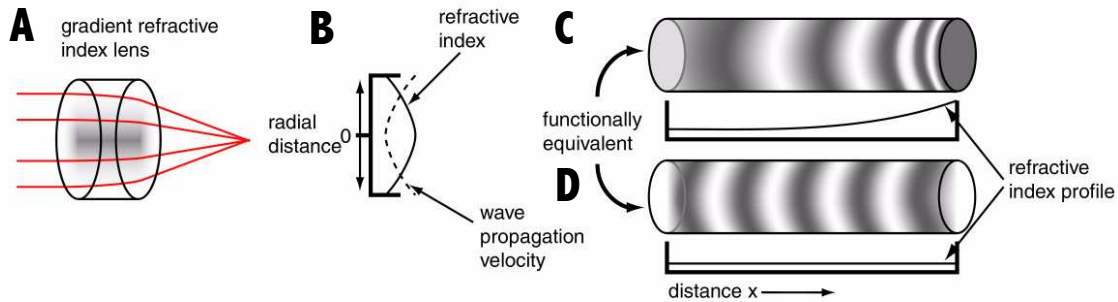


Figure 3.13. A: A gradient refractive index (GRIN) lens whose refractive index varies B: as a function of distance from its cylindrical axis with a parabolic or exponential gradient refractive index profile. C: If a cylindrical resonator with a nonlinear GRIN profile is used as a resonator, the standing waves that it sustains will be correspondingly distorted by the GRIN, although the resonance will be functionally equivalent to D: an undistorted resonance in a resonator with a constant, or uniform GRIN profile.

the direction of the greater refractive index, allowing a cylinder of glass with plane end-faces to behave like a convex lens, bending a parallel beam of light to a focal point. A reverse gradient with lower refractive index at the center than the periphery, would behave like a concave lens that makes a parallel beam of light diverge. A gradient refractive index in a resonator, for example using a GRIN lens as a lasing cavity, would also distort any standing wave that it sustains. Figure 3.13 C shows a standing wave along a cylindrical resonator whose gradient refractive index profile varies along the length of the cylinder, with lower refractive index and thus greater propagation velocity, to the left, increasing in nonlinear fashion towards the right. The standing waves in that resonator would be distorted by this change in the propagation velocity in such a way that the shorter waves towards the right in the figure oscillate back and forth at the same temporal frequency as the longer waves towards the left, and thus, all the waves oscillate in perfect synchrony along the length of the resonator despite their differences in size. This squashed non-periodic pattern is thus *functionally equivalent* to a much longer un-squashed waveform in a uniform resonator with the same number of peaks and troughs, as suggested in Figure 1.13 D.

The possibility of imposing a regular distortion on the shape of the standing wave in a non-uniform resonator opens a unique opportunity to circumvent the boundary conditions at the boundaries of a resonator, and thus liberate the resonances within from the strict constraints of the geometry of the resonator. This in turn offers an opportunity to create resonances that are not strictly constrained by the geometry of the resonator's bounding limits. The refractive index of a wave propagating material is a consequence of a time delay in the propagation. In the case of light travelling through glass, the time delay is due to the absorption, and

subsequent re-emission of each photon of light many times as it passes through the material, effectively increasing the light path length to include a few orbits around each atomic nucleus that it encounters along its path. This slow-down in light propagation refracts a beam of light by the same principle that a column of marching soldiers is deflected if it enters obliquely into a region of increased walking resistance, a ploughed field or low brush, which slows the column on one side before the other, deflecting its path toward the denser medium. In theory there is no limit to the magnitude of refractive index, up to an infinite refractive index, which describes a perfectly opaque material (light goes in but never comes out). In fact light itself has even been slowed down to bicycle speed in this manner, by using a Bose-Einstein condensate to delay the light in random fluctuations back and forth within the condensate before eventual re-emission. In a biological medium, whether chemical reaction-diffusion, or electrochemical oscillations, it is perfectly possible to create a system with very large, up to infinite refractive index using less exotic means than a Bose-Einstein condensate. In a theoretical model this is easily achieved by simply adding the appropriate time delay to the wave propagation equation.

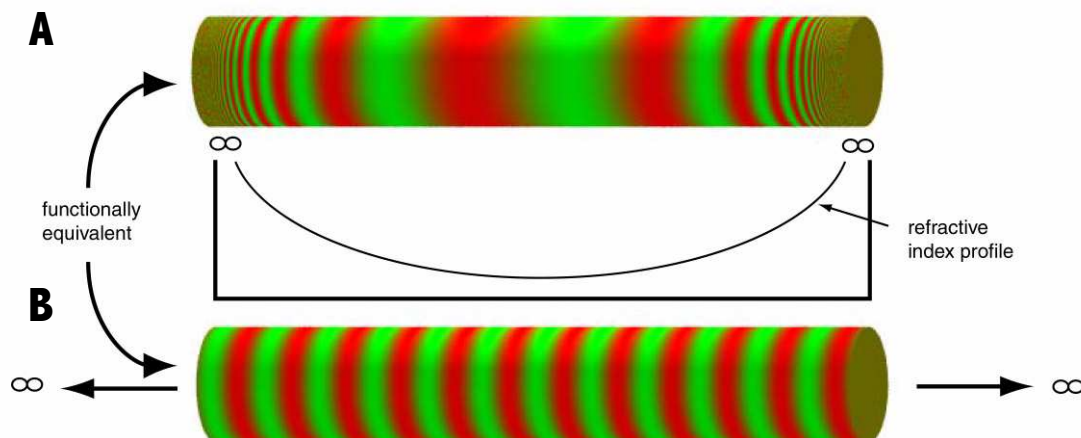


Figure 3.14. A: A resonator whose GRIN profile reaches infinity at the ends, will sustain standing waves with an “infinite” number of nodes towards the ends, which is functionally equivalent to B: a resonance in a uniform resonator of infinite extent, which is a physical impossibility.

Figure 3.14 A shows a cylindrical resonator with a rather extreme gradient refractive index profile that is relatively low at the center (high propagation velocity) but rises to an infinite refractive index at the two ends, or zero propagation velocity. Actually, it is not necessary for the refractive index to be truly infinite, it is sufficient to make it just very large, which is tantamount to “practically infinite” within some temporal window either side of the center. A wave

propagating from the center outwards towards the ends, would propagate ever slower as it approached the ends, but never quite get there, (or only after a very long time) successive wave fronts piling up on each other like traffic slowing for a traffic jam. It is perfectly possible to set up self-amplifying standing waves in a resonator with this peculiar property. But since the refractive index is practically infinite at the ends of the resonator, the resonance is functionally equivalent (to some approximation) to an infinite resonance in an infinitely long resonator, as suggested in Figure 3.14 B. The use of a practically infinite refractive index, which is a physical *possibility*, allows the construction of something that is functionally equivalent to an amplified resonance in an infinitely long resonator, with an infinite number of nodes along its infinite length, something that is physically *impossible*. Of course the “trick” here is that there are not really an *infinite* number of nodes in the standing wave, there are nodes that get ever smaller and more compressed towards the ends, but in a real physical system this would only occur to some smallest scale, beyond which there would be no more vibrational nodes. Nevertheless, this “trick” has the effect of removing the effect of the abrupt bounding limits of the resonator, in a pattern that emulates the kinds of resonances that could emerge in an infinitely long resonator, but expressed in a finite bounded representation.

The standing waves in a normal finite length resonator are constrained by the boundary conditions at the ends. If the ends of a tube are closed, then vibrational nodes will form at the ends due to reflections back from the closed end. The waveform in the resonator is phase-locked to its ends. In the functionally infinite resonator depicted in Figure 3.13, on the other hand, there is no discrete end point to the resonator, and thus the wave that emerges spontaneously in a self-amplifying resonance is not constrained to a single phase, but can appear at any phase. In other words, the wave pattern shown in Figure 3.14 A, which exhibits an asymmetrical *sine* function across the center, with negative to the immediate left of center and positive to the right, could be phase-shifted 90 degrees to a *cosine* function, positive across the center and negative to the immediate right and the left, or it could be shifted to any intermediate phase value, while remaining balanced in resonance terms. That is, each of those phase-shifted waveforms would be equally valid or sustainable as standing waves in that resonator, and thus this resonator has become invariant to the phase of the waveforms that it sustains. It is a phase-invariant representation of waveforms in that space, in the sense that a tuned resonator tuned to the frequency of that wave would resonate to the wave regardless of its phase. This phase invariance also confers a

frequency invariance to the standing waves that can appear in the tube. In a finite and bounded resonating cylinder with uniform refractive index profile, the standing waves that can be sustained are restricted to the frequency of the fundamental, and its infinite series of higher harmonics. The infinite bounded resonator, on the other hand, can sustain waveforms of any frequency equally, (within some lower and higher limits) and thus this resonator is both invariant to frequency and phase of the waveforms that it can sustain in self-amplified resonance. The resonator has broken free of the boundary conditions imposed by the discrete ends of the resonating system. The effect of the gradient refractive index is to insulate the resonances at the center from the boundary conditions at the ends, in the same way that a window function, like a *hanning window*, is used in Fourier filtering operations in image processing in order to eliminate the “ringing” due to the abrupt boundaries of the image, allowing a finite sized image to be treated as a finite sample of an infinite repeating pattern. This principle could be easily demonstrated by standing wave vibrations in a “gradient refractive index” slinky that is devised to have progressively increasing mass and stiffness towards one end of the spring, which is then fixed to a rigid attachment point. Normally, the waves that travel to an attachment point are reflected back in mirror-fashion from the abrupt transition of stiffness at the attachment point. In the gradient refractive index slinky, the transition is no longer abrupt, but continuous, and thus a wave propagating towards the end is reflected back continuously as it traverses the region of increasing refractive index, thus distributing the reflection process throughout a continuous region of the spring, and thus liberating the vibrations of the spring from the strict constraints of the abrupt boundary. The consequences of this principle extended into two- or three-dimensional resonances are even more dramatic.

### **The Infinite Bounded Sphere**

The concept of a functionally infinite resonator can be extended into two or three dimensions by creating a circular, or spherical resonator with a gradient refractive index that goes to infinity at the bounding limits of the resonator. Figure 3.15 A shows a standing wave resonance in a resonator with this “infinite bounded” property. This figure can be viewed as either a flat circular disk, like a circular Chladni plate with a gradient refractive index profile, or as a central great circle slice through a three-dimensional spherical resonator with a three-dimensional gradient refractive index profile. In either case, the speed of wave propagation varies continuously with distance from the center such that it takes equal time for a wave propagating outward from the center to cross each of the concentric shells

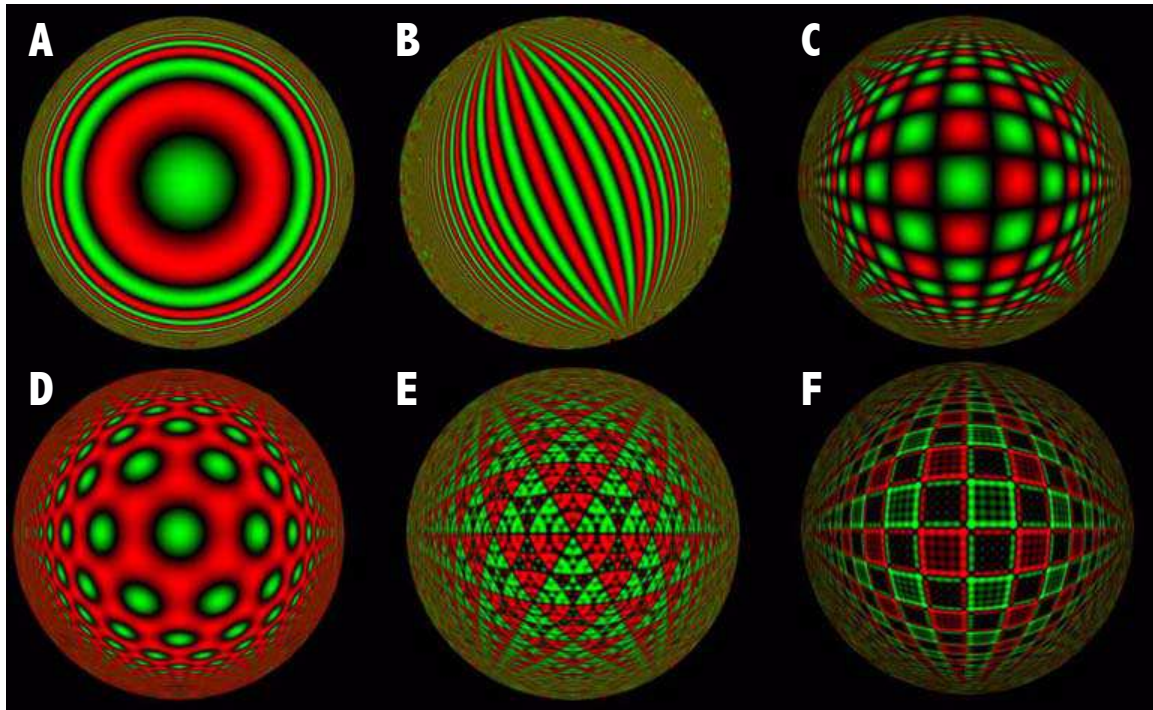


Figure 3.15. Standing wave resonance patterns viewed in cross-section of an infinite bounded sphere in which the refractive index varies with distance from the center, reaching infinite refractive index (zero wave propagation velocity) at the bounding surface of the sphere. A: Concentric pattern. B: Linear perspective pattern. C: Checkerboard pattern. D: Hexagonal pattern. E: Higher harmonics on a hexagonal pattern. F: Higher harmonics on a checkerboard pattern.

delimited by the depicted waveform, travelling faster across the rings near the center, and ever slower towards the periphery, slowing to a complete stop just as it reaches the outer boundary. This confers an additional “momentum” or functional inertia to the standing waves out toward the periphery, that allows a thinner compressed ring of the standing wave toward the periphery to resonate in balance with a thicker expanded ring nearer the center, as if they were waves of exactly the same size and shape balanced symmetrically against each other in a uniform resonator. As in the case of the GRIN resonator depicted in Figure 3.13 E, this resonator can sustain standing waves of any frequency within a range of frequencies between some lower and upper limits, and of any phase shift. But the full circular, or spherical closure of the infinite bounded sphere confers yet another invariance to this representation, an invariance to the shape of the resonator, a property that is highly desirable in a perceptual representation. Figure 3.15 B shows another standing wave resonance that would be sustained in the infinite bounded resonator, in this case a pattern of parallel sinusoidal waves at some orientation. Again, the smaller waves toward the periphery remain in dynamic balance with the larger waves through the center, but there is now a spatial distortion imposed on the standing waves, due to the redefinition of distance as a function of wave propagation velocity, that bends the parallel wave fronts into

graceful arcs that meet at a pair of “vanishing points” in opposite directions across the resonator. In other words, this standing wave resonates in the same pattern as a field of straight parallel waves that extend to infinity in all directions, except expressed in a finite bounded representation. This resonator is now totally invariant to the shape of the standing waves that it sustains, because they no longer need to vibrate in balance with respect to the reflective boundaries of the resonator, but rather, the waves that emerge in this resonator must merely be balanced with respect to themselves, balancing the positive portions of the wave pattern against equal and opposite negative portions of the wave, a resonance of the similarity of the wave to itself, in either simple, or compound hierarchical form, rather than to the shape of the resonator. This representation now encodes two completely different kinds of spaces, all in a single representation. One is the spherical bounded and finite space of the resonator mechanism itself, that has a finite size, the other is a functionally infinite space (expressed to a finite resolution) in which distance is defined not by physical distance, but by the time taken to traverse it at the speed of wave propagation through the medium. The world defined by the waves themselves is an undistorted Euclidean world of practically infinite extent, although with a finite spatial resolution that falls off to zero at the periphery. It turns out that this infinite bounded world has the same geometrical distortions as the world of our perceptual experience.

Figure 3.15 C shows another standing wave that would be sustained in the infinite bounded resonator, this one composed of two sets of parallel sinusoids oriented at right angles to each other, creating a checkerboard pattern of waves, that are also symmetrically balanced against each other, with exactly the same magnitude of positive and negative values across the pattern of a whole. Figure 3.15 D shows a hexagonal grid defined by three sets of parallel waves oriented at 120 degrees to each other, again maintaining a perfect balance of the wave against itself. These patterns could be sustained at any frequency through a range of frequencies, at any phase, and at any orientation through the resonator. The infinite bounded resonator is not confined to waves of sinusoidal form, but it can also resonate to patterns composed of fundamental wave forms and an orderly series of higher harmonics, to define patterns of arbitrary complexity. Figure 3.15 E and F show just two of an infinite number of possible combinations of wave patterns and their higher harmonics, with the higher harmonics expressed as integer multiples of some selected fundamental frequency representing the base pattern. Each one of the infinite array of possible patterns that can be composed of periodic patterns of sinusoids and their higher harmonics, are the natural modes of resonance of the

infinite bounded resonator. That is, they express standing waves that would be sustained by self-amplification in the resonator if that pattern were imposed as an initial condition. Unlike the resonance of Falstad's box mode applet, this resonator is tuned to resonate to any pattern that has the self-similar property of either symmetry, or periodicity, or both, in some combination.

If a resonator of this sort is associated with a bank of tuned resonators, as suggested in Chapter 2 with the analogy of a bank of organ pipes, the tuned resonators would respond to their characteristic waveforms independent of rotation and translation of the pattern, and also to some extent invariant to spatial scale. For example the periodic striped pattern in Figure 3.14 B, oscillates at a single frequency characteristic of the scale of the waveform because the broad waves through the center vibrate at exactly the same frequency as the narrower waves in the periphery. A similar pattern of parallel waves that are either broader or narrower as they pass through the center, would produce a different characteristic vibration frequency that is either lower or higher in temporal frequency respectively. In other words, the temporal frequency represents the absolute scale of the pattern, even though the scale also varies from the center to the periphery. This is the property of harmonic resonance that accounts for the extraordinary invariance in visual perception and recognition to rotation, translation, and scale, as well as for the distortions of visual perspective, that have been so resistant to explanation in more conventional neural network terms.